Available online at www.sciencedirect.com
SCIENCE DIRECT®

ELSEVIER

Coastal Engineering 49 (2003) 71–81

Coastal Engineering
An International Journal for Coastal, Harbour and Offshore Engineers

www.elsevier.com/locate/coastaleng

Internal generation of waves in 2D fully elliptic mild-slope equation FEM models

Giorgio Bellotti[a], Gian Mario Beltrami[b], Paolo De Girolamo[b,*]

[a] Dipartimento di Scienze dell'Ingegneria Civile (DSIC), Università di Roma Tre, via Vito Volterra 62, Rome 00146, Italy
[b] Dipartimento di Ingegneria delle Strutture, delle Acque e del Terreno (DISAT), Università degli Studi di L'Aquila, Monteluco di Roio, L'Aquila 67040, Italy

Received 8 November 2002; received in revised form 29 April 2003; accepted 2 June 2003

Abstract

This paper looks at an alternative approach for the treatment of open boundaries in linear wave field simulations by means of fully elliptic mild-slope equation (MSE) finite elements models. In these kinds of models, the domain of investigation is traditionally contoured both by reflecting–absorbing boundaries, which simulate the coastline or the structures that emerge from the sea, and by an 'open' or 'artificial' boundary, which separates the sea region included in the domain from the semi-infinite region that extends outward to infinity. The approach presented here assumes the domain to be completely contoured by reflecting–absorbing boundaries. A total absorbing boundary is, in particular, assumed to separate the inner (finite) from the outer (semi-infinite) sea region. Sources of energy, which generate waves of specified height and period, are located within the domain along a line in the proximity of the inner–outer sea region boundary. Reflected and scattered waves can propagate over the generation line and are absorbed at the open boundary. Numerical tests have been carried out to simulate progressive and stationary waves in a channel and long waves around a fully reflecting circular island on a parabolic shoal, and to evaluate the amplification factors of a long and narrow bay. All these validation tests show a very good agreement with the available analytical solutions. A discussion is finally carried out on the advantages and disadvantages of the presented approach with respect to traditional ones.
© 2003 Elsevier B.V. All rights reserved.

Keywords: Mild-slope equation; Internal wave generation; Open boundary conditions; Absorbing boundary conditions; Elliptic model

1. Introduction

Linear wave field simulation by means of mild-slope equation (MSE) models still plays an important role in resolving coastal engineering problems. Taking into account the combined effects of reflection, refraction, and diffraction actually makes the models, based on the equation derived by Berkhoff (1972, 1976), an excellent means to model linear water wave propagation towards harbors and coastal regions. Furthermore, the inclusion of a dissipation factor (Booij, 1981) has made it possible to improve the performance of these models by taking into account the effects of phenomena such as bottom friction (Dalrymple et al., 1984; Chen, 1986; Kostense et

* Corresponding author.
E-mail address: paolo.degirolamo@uniroma1.it (P. De Girolamo).

0378-3839/03/$ - see front matter © 2003 Elsevier B.V. All rights reserved.
doi:10.1016/S0378-3839(03)00047-4

al., 1986) and wave breaking (Battjes and Janssen, 1978; Dally et al., 1985; De Girolamo et al., 1989; Zhao et al., 2001; Beltrami et al., 2001).

This paper looks at an alternative approach for the treatment of the 'open' boundaries in fully elliptic MSE finite element models (FEMs) such as the widely known HARBD (Chen and Houston, 1987; Chen and Mei, 1974; Mei, 1983; Thompson and Hadley, 1995; Thompson et al., 1996), PHAROS (Delft Hydraulic Laboratory, 1985a,b; Dingemans, 1997), and CGWAVE (Xu et al., 1996; Demirbilek and Panchang, 1998).

In these kind of models, the domain of investigation is traditionally contoured both by reflecting–absorbing boundaries, which simulate the coastlines or the structures that emerge from the sea, and by an 'open' or 'artificial' boundary, which separates the sea region included in the domain from the semi-infinite region that extends outward to infinity. As it is known, at the 'open' boundary, both incoming reflected and scattered waves coexist. In order to ensure the continuity of the free surface elevation at this boundary, as well as of the velocity component normal to it, the potential of these waves is usually given in terms of an a priori chosen mathematical expression, which holds under specific assumptions.

Along the 'open' boundary, for example, the incoming wave velocity potential can be expressed as that of a progressive wave only in the case that the boundary itself falls within a sea region of constant depth. In the case of a sloping beach, both height and direction of the incoming wave vary from point to point along the lateral side of this boundary. The potential should be therefore calculated at each of these points. For simplicity, only the problem of treating 'open' boundaries on constant depth is considered in the present paper, with the extension to the variable depth case left to further developments.

Assuming that the velocity potential of the incoming wave is equal to that of a progressive wave, which propagates on a constant depth sea region, leaves unchanged the problem of expressing the scattered and reflected wave velocity potential. The amount of the reflected wave energy, which propagates back towards the 'open' boundary and then outward to infinity, is in fact not known a priori, depending on the solution of the problem itself. In order to solve this major problem, the traditional approach has been that of representing the reflected and scattered wave velocity potential by means of some a priori chosen mathematical expression.

Several authors (Xu et al., 1996; Kostense et al., 1986; Chen, 1986) have described the reflected waves as plane waves. Nevertheless, this representation actually holds under the following assumptions: (a) constant depth of the outer sea region, (b) collinear coastlines, (c) coastlines characterized by a single reflection coefficient, and (d) nonbreaking wave field.

The most used mathematical representations of the scattered wave velocity potentials φ_s are based on line integral of the appropriate Green function (Berkhoff, 1972, 1976) or Hankel function series (Chen and Houston, 1987; Chen and Mei, 1974; Mei, 1983). Recently, Xu et al. (1996) have proposed an expression of φ_s that relaxes some of the hypothesis on which are based the previous representation. Although the cited representations can be extremely effective, they do not have general validity. Care should therefore be used in applying this approach for simulating complex wave fields characterized by not well-known scattering and reflection sources, as well as by wave breaking.

A way to bypass these problems can be that of generating the incoming waves inside the computational domain and absorbing the outgoing waves at the boundary that separates the inner finite from the outer semi-infinite sea region. Internal wave generation was originally proposed by Larsen and Dancy (1983) in the framework of the Boussinesq-type equations. These authors showed that including a source function in the mass conservation equation and modulating it in time makes it possible to generate periodic waves inside the computational domain. Furthermore, Larsen and Dancy showed that it is possible to absorb all the outgoing wave energy by means of a so-called 'sponge layer' (i.e., a numerical tool able gradually to damp wave energy before it is reflected at the 'open' boundaries).

To the present authors' knowledge, this approach, which is commonly used in time-marching numerical models based on the hyperbolic MSE (Copeland, 1985; Madsen and Larsen, 1987; Lee and Doug Suh, 1998) and on the Boussinesq-type equations (Wei et al., 1999), has never been used in fully elliptic wave models.

The approach presented in the present paper assumes the domain to be completely contoured by reflecting–absorbing boundaries. A totally absorbing boundary is, in particular, assumed to separate the inner (finite) from the outer (semi-infinite) sea region. Sources of energy, which generate waves of specified height and period, are located—within the domain—along a line in the proximity of the inner–outer sea region boundary. Reflected and scattered waves can propagate over the generation line and are absorbed at the open boundary. Using this kind of approach in fully elliptic MSE–FEM models shifts their main problem from that of correctly representing the wave velocity potential at the 'open' boundary to that of perfectly absorbing the outgoing wave energy. As recently shown by Steward and Panchang (2000) and Beltrami et al. (2001), total absorption at boundaries can be effectively achieved by means of iterative techniques.

The present paper provides the derivation of the source term, which can be included in the MSE to generate waves inside the computational domain, together with the results of the numerical tests carried out in order to validate the proposed approach by means of the GEMMA FEM model (De Girolamo and Sammarco, 1993, Beltrami et al., 1998, 2001). In particular, the validation tests are concerned with the simulation of progressive and stationary waves in a channel and long waves around a fully reflecting circular island on a parabolic shoal, and the evaluation of the amplification factors of a long and narrow bay. Being very demanding with respect to the treatment of the 'open' boundary makes the circular island and the harbor resonance tests particularly suitable to show the actual efficiency of the presented approach.

A discussion is finally carried out on the advantages and disadvantages of the presented approach with respect to traditional ones.

2. Model formulation

2.1. The MSE with a source term

The fully elliptic form of the MSE with the inclusion of the internal wave generation term (ψ) can be expressed as:

$$\nabla \cdot (cc_g \nabla \varphi) + \omega^2 \frac{c_g}{c} \varphi = \psi \tag{1}$$

where c and c_g are the phase and group celerity, respectively; φ is the complex wave velocity potential; ω is the angular frequency; and k is the wave number, once a Cartesian reference frame is considered. In order to discuss the role of ψ and to introduce a convenient expression for this term, the MSE (1) is usefully derived from the modified form suggested by Copeland (1985), that is,

$$\frac{\partial \eta}{\partial t} + \frac{c}{c_g} \nabla \cdot \mathbf{Q} = 0 \tag{2}$$

$$\frac{\partial \mathbf{Q}}{\partial t} + cc_g \nabla \eta = 0 \tag{3}$$

where η is the real surface elevation and $\mathbf{Q}$ is a pseudoflux, which, in the case of deep or constant water depth, coincides with $c_g\eta$ (for more details, refer also to Madsen and Larsen, 1987).

Internal wave generation is traditionally achieved by periodically adding and subtracting mass to the system (i.e., modifying the mass equation (Eq. (2)) as follows:

$$\frac{\partial \eta}{\partial t} + \frac{c}{c_g} \nabla \cdot \mathbf{Q} = S e^{-i\omega t}. \tag{4}$$

In Eq. (4) $i = \sqrt{-1}$, and only the real part of the equation is taken into account. The term S is equal to zero everywhere except along the wave generation line, while its magnitude, which is constant in time, is to be chosen in order to obtain the specified wave height.

In a hyperbolic wave model, the absorption of the outgoing waves at the 'open' boundary is obtained by introducing a dissipative effect in the momentum equation, i.e., by expressing Eq. (3) as:

$$\frac{\partial \mathbf{Q}}{\partial t} + cc_g \nabla \eta = -\epsilon \mathbf{Q}. \tag{5}$$

It should be noticed that $\epsilon = 0$ except in the regions close to the open boundaries (sponge layers). It is shown in Section 2.2 that, in fully elliptic models, such an absorption can be effectively achieved by means of the imposition along the 'open' boundary of a total absorption condition.

Assuming that ϵ does not vary in space, and eliminating $\mathbf{Q}$ from both the mass (Eq. (4)) and momentum (Eq. (5)) equations gives:

$$\frac{\partial^2\eta}{\partial t^2} = \frac{c}{c_g}\nabla\cdot(cc_g\nabla\eta) - \epsilon\frac{\partial\eta}{\partial t} - i\omega S e^{-i\omega t} \tag{6}$$

which is the equation of a harmonically excited wave propagating with given phase and group celerity c and c_g, and in which damping is represented by the term $\epsilon\partial\eta/\partial t$. For simplicity's sake, it is convenient to assume uniformity along the y-axis (i.e., independence of y) as well as constant water depth. This simplifies Eq. (6), which can be expressed as:

$$\frac{1}{c^2}\frac{\partial^2\eta}{\partial t^2} = \frac{\partial^2\eta}{\partial x^2} - \frac{\epsilon}{c^2}\frac{\partial\eta}{\partial t} - \frac{i\omega S}{c^2}e^{-i\omega t} \tag{7}$$

where the amplitude S of the source term is equal to zero everywhere except along a line parallel to the y-axis. Assuming, without loss of generality, that the generation line is $x=0$ makes it possible to represent the amplitude S of the source term by means of a delta function $\delta(x)$ (Mei, 1995, p. 105) and therefore to express Eq. (7) as:

$$\frac{1}{c^2}\frac{\partial^2\eta}{\partial t^2} = \frac{\partial^2\eta}{\partial x^2} - \frac{\epsilon}{c^2}\frac{\partial\eta}{\partial t} - \delta(x)\frac{i\omega S}{c^2}e^{-i\omega t}. \tag{8}$$

For very small ϵ, it is possible to realize a weak damping of the generated waves and therefore to satisfy the radiation condition (Mei, 1983, pp. 113–116).

An analytical solution of Eq. (8) can be obtained by means of a Fourier transform technique (Mei, 1995, pp. 247–250). This solution consists of two progressive waves of amplitude A=S/(2c), which emanate from the generation line. These waves, for $\epsilon\to 0$, can be expressed as:

$$\eta(x,t) = \frac{S}{2c}e^{i(k|x|-\omega t)}. \tag{9}$$

Going back to Eq. (6) with $\epsilon=0$ and assuming that the generation line coincides with the y-axis make it possible to express the wave equation as:

$$\frac{\partial^2\eta}{\partial t^2} = \frac{c}{c_g}\nabla\cdot(cc_g\nabla\eta) - i\omega 2cA\delta(x)e^{-i\omega t}. \tag{10}$$

Assuming a harmonic variation of η and using the complex wave velocity potential φ (i.e., $\eta(x,y,t)$= $[(-i\omega)/(g)]\varphi(x,y)e^{-i\omega t}$) make it possible—by multiplying Eq. (10) for $(c_g/c)e^{i\omega t}$—to obtain the elliptic form of the MSE, that is,

$$\nabla\cdot(cc_g\nabla\varphi) + \omega^2\frac{c_g}{c}\varphi = 2c_g i\omega\tilde{\varphi}\delta(x) \tag{11}$$

where $\tilde{\varphi}$ is the complex velocity potential of the generated wave that can be expressed as

$$\tilde{\varphi} = -\frac{g}{i\omega}a \tag{12}$$

where a is the real wave amplitude.

Direct comparison with Eq. (1) shows that a simple expression for the source function $\psi=2c_g i\omega\tilde{\varphi}\delta(x)$ has been found. This ensures that the amount of mass added to the system along the (straight) generation line is such that on an horizontal bottom, two progressive waves with real amplitude a are generated. It is clear that if the generation line is placed on a sloping bottom, the generated wave amplitude changes due to shoaling, refraction, and reflection effects.

It is easy to show that in the case of constant water depth, Eq. (11) reduces to the well-known Helmhotz equation with a source function, which reads:

$$\nabla^2\varphi + k^2\varphi = 2ik\tilde{\varphi}\delta(x). \tag{13}$$

2.2. Boundary conditions

The formulation of the model proposed in the present paper assumes that the domain of investigation is totally contoured by reflecting–absorbing boundaries. Along these boundaries, a reflection condition must be therefore imposed. This condition is expressed as:

$$\frac{\partial\varphi}{\partial n} + b\varphi = 0 \tag{14}$$

where n is taken along the normal to the boundary and $b=b_1+ib_2$ is the complex reflection coefficient, which, assuming no phase shift between the reflected and the incoming wave, can be expressed as:

$$b_1 = 0, \quad b_2 = -k\cos(\beta)\frac{1-R}{1+R} \tag{15}$$

where R is the real reflection coefficient, and β is the angle between the normal to the wave crest and the normal to the boundary (Beltrami et al., 2001). The partial reflection condition is therefore a function of β, and its efficiency depends on the accuracy of the given value of the incidence angle. Actually, it has been demonstrated (Behrendt, 1985) that the farther β is from its true value, the greater the extent to which undesired reflections affect the domain. Behrendt (1985) has also shown that of all the absorption–reflection conditions ($0 \le R \le 1$), the total absorption condition ($R=0$) is the one that is most affected by inaccuracies of the estimated value of β. In a topographically complex domain, β is not known a priori; therefore, it is an unknown function of the wave parameters and of the geometry of the domain. Nevertheless, it has been shown that an iterative procedure can be efficiently applied in order to deal with the indeterminacy of β both in the general partial reflection case (Isaacson and Qu, 1990; Steward and Panchang, 2000) and in the specific total absorption case (Beltrami et al., 2001).

2.3. FEM representation

The weak formulation on which the GEMMA FEM model is based can be expressed as:

$$0 = \int\int_{\Omega} \left[cc_{\mathrm{g}} \nabla v \nabla \varphi - \omega^2 \frac{c_{\mathrm{g}}}{c} v\varphi + 2vc_{\mathrm{g}} i\omega\tilde{\varphi}\delta(x) \right] \mathrm{d}\Omega + \int_{\partial\Omega_{\mathrm{R}}} cc_{\mathrm{g}} bv\varphi \mathrm{d}(\partial\Omega_{\mathrm{R}}) \quad (16)$$

where $v(x,y)$ is a test function that can be viewed as a variation in φ that satisfies the essential boundary condition. The first integral extends over the computational domain Ω and the second one over its boundary ($\partial\Omega_{\mathrm{R}}$).Since:

$$\int_{-\infty}^{\infty}\int_{-\infty}^{\infty} f(x,y)\delta(x)\mathrm{d}x\mathrm{d}y = \int_{\Gamma_{\mathrm{G}}} f(x,y)\mathrm{d}\Gamma_{\mathrm{G}} \quad (17)$$

the third term in the first integral reduces to a line integral to be evaluated on the internal wave generation line Γ_{G}, which is parallel to the y-axis. The final weak formulation on which the model is based is therefore given by:

$$0 = \int\int_{\Omega} \left[cc_{\mathrm{g}} \nabla v \nabla \varphi - \omega^2 \frac{c_{\mathrm{g}}}{c} v\varphi \right] \mathrm{d}\Omega + \int_{\Gamma_{\mathrm{G}}} 2vc_{\mathrm{g}} i\omega\tilde{\varphi}\mathrm{d}\Gamma_{\mathrm{G}} + \int_{\partial\Omega_{\mathrm{R}}} cc_{\mathrm{g}} bv\varphi\mathrm{d}(\partial\Omega_{\mathrm{R}}). \quad (18)$$

Usual techniques of FEM with triangular elements are used to represent the MSE as a system of linear algebraic equations, which, in particular, has a complex banded coefficient matrix.

3. Validation tests

As already stated, the validation tests have been run to simulate progressive and stationary waves in a channel (Section 3.1) and long waves around a fully reflecting circular island on a parabolic shoal (Section 3.2), and to evaluate the amplification coefficients of a long and narrow bay (Section 3.3). Being very demanding with respect to the treatment of the 'open' boundary makes the circular island and the harbor resonance tests particularly suitable to show the actual efficiency of the presented approach.

3.1. Progressive and stationary waves in a channel

A long and narrow channel was used to simulate progressive and stationary waves (Fig. 1). The 20-m long and 0.2-m wide channel is discretized by a mesh of 603 nodes and 800 equal triangular right-angled elements with sides of 0.1 m. A constant depth of 0.701 m has been used.

A monochromatic wave of height $H=0.1$ m and period $T=1.5$ s is generated at a line located in the middle of the channel, and propagates towards both the left and the right ends of the channel. A total absorp-

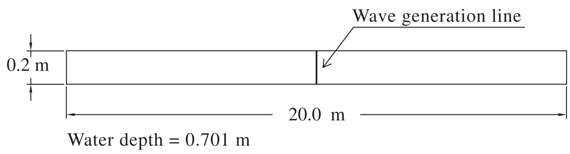

Fig. 1. Long and narrow channel definition sketch.

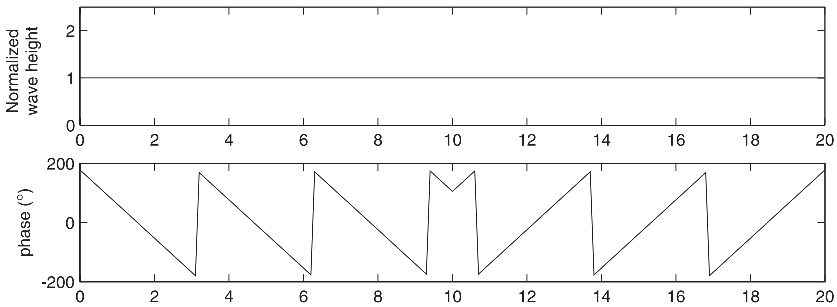

Fig. 2. The 1D progressive wave.

tion condition ($R=0$) has been imposed at both ends of the channel in the progressive wave simulation test, whilst a total reflection ($R=1$) and a total absorption condition ($R=0$) have been, respectively, imposed at the left and right ends for the stationary wave case. A total reflection condition ($R=1$) is imposed at the lateral side of the channel in both simulations.

Figs. 2 and 3 show the result of the progressive wave simulation test and of the stationary wave simulation, respectively. The results are presented in terms of wave height normalized with respect to the desired one (upper panels in the figures) and phase (lower panels). As expected, Fig. 2 shows two progressive waves of the desired height emanating from the middle of the channel at which the generation line is located.

Fig. 3 shows that a stationary wave is established in the left side of the channel, whilst a progressive wave propagates in its right side. Furthermore, the figure clearly shows that the wave energy reflected back at the left end of the channel propagates over the generation line and superposes to the progressive wave. For what concerns the height of waves at the right of the generation line, it depends on the phase of the two wave systems; for the specific case at hand, the resulting wave height is about 0.6 times the height of the generated wave. It is worth mentioning that changing the geometrical dimensions of the channel (i.e., its length, width, and depth), as well as the characteristics of the simulated monochromatic wave (i.e., its height and period), does not change the validity of the results, which are always those expected. In the test with progressive wave, the wave height is equal to the expected one up to five decimal figures. This small discrepancy can be imputed to numerical integration errors.

3.2. Circular island

The definition sketch of the circular island test is shown in Fig. 4. A fully reflecting circular island with radius $r_1=10{,}000$ m is placed on a parabolic shoal, which extends up to a distance of $r_2=30{,}000$ m from the center of the island. A sea region of constant water depth $h_2=4000$ m, which extends outwards to infinity, is assumed to surround both the island and the shoal. The shoal water depth is a

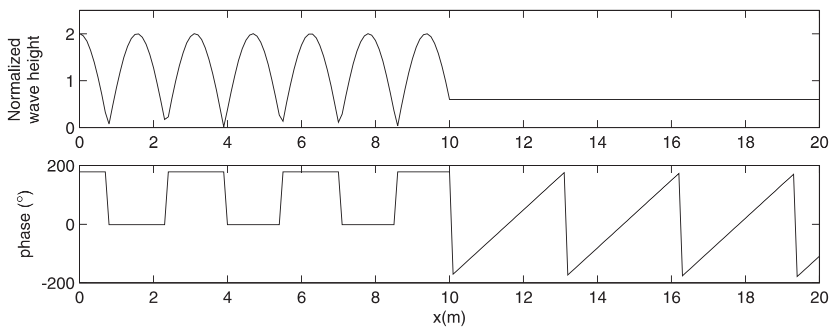

Fig. 3. Left side of the domain: 1D stationary wave; right side of the domain: 1D progressive wave.

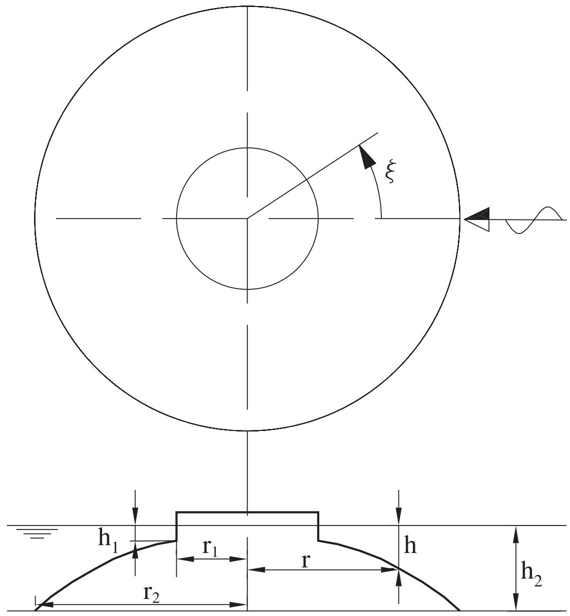

Fig. 4. Definition sketch of circular island on a paraboloidal shoal.

function of the distance from the center of the island, and is expressed as $h(r)=(h_2/r_2^2)r^2$. The water depth at the island coastline is therefore approximately equal to 444 m.

A square domain with sides of 130,000 m has been used to carry out this test (Fig. 5). In particular, the calculation domain (the island being placed exactly in the middle) is discretized by 3568 nodes and 6848 elements. A wave of height $H=1$ m and period $T=240$ s is generated at a line located—within the domain—500 m from the right boundary. A total absorption condition ($R=0$) is imposed on the four-side 'open' boundary, which separates the sea region included in the domain from the infinite region that extends outward to infinity. The waves reflected by the island or those refracted by the shoal are initially assumed to propagate normally to the 'open' boundary, and the iterative procedure proposed by Beltrami et al. (2001) is used to deal with the angle β indeterminacy of the total absorption condition (Section 2.2). A total reflection condition ($R=1$) is then imposed along the island coastline.

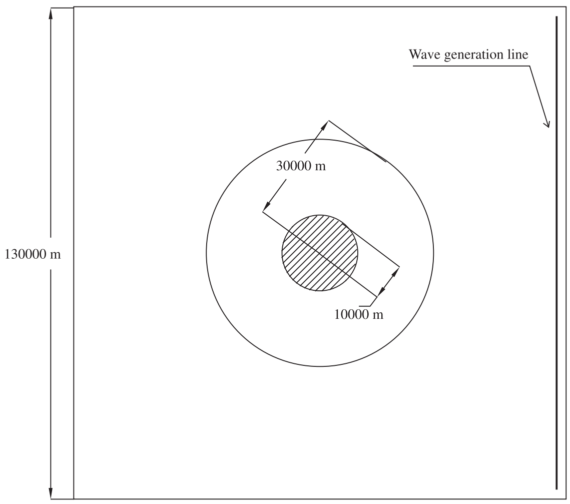

Fig. 5. Calculation domain for the circular island test.

The numerical test result is compared with the analytical solution derived by Homma (1950) and Jonsson et al. (1976), which can be expressed as:

$$\frac{\zeta}{A_\mathrm{i}} = \sum_{n=0}^{\infty} \frac{\frac{2}{\pi}\epsilon_n i^{n+1}\rho\left[\left(\frac{r}{r_1}\right)^{-1+\alpha_n} + \frac{\alpha_n-1}{\alpha_n+1}\left(\frac{r}{r_1}\right)^{-1-\alpha_n}\right]\cos(n\xi)}{\rho^{\alpha_n}\left[(1-\alpha_n)H_n+\tau H_n'\right]+\rho^{-\alpha_n}\frac{\alpha_n-1}{\alpha_n+1}\left[\tau H_n'+(1+\alpha_n)H_n\right]} \tag{19}$$

where A_i is the incident wave amplitude, ϵ_n is the Jacobi symbol (i.e., $\epsilon_n=1$ for $n=0$ and $\epsilon_n=2$ for $n\neq$

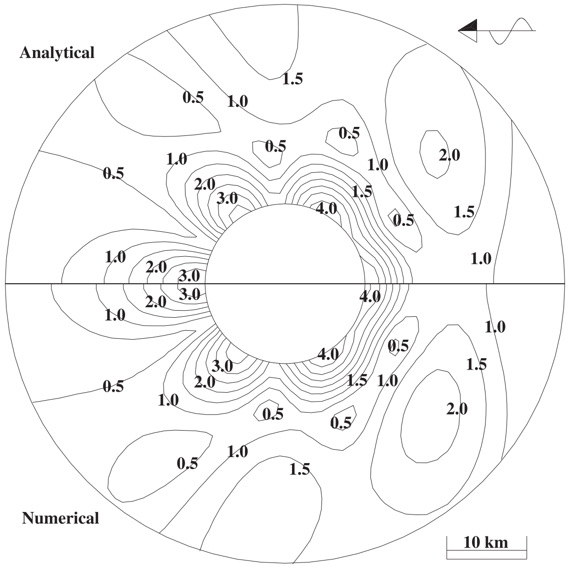

Fig. 6. Wave height contours; comparison between analytical (above) and numerical (below) solution.

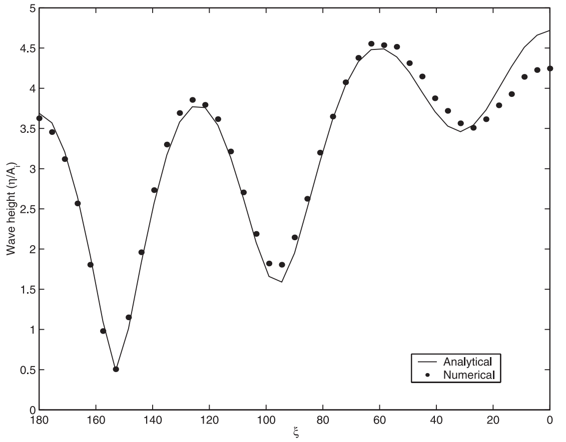

Fig. 7. Wave height along island wall; comparison between analytical (solid line) and numerical (dots) solution.

0, $\rho = r_2/r_1$, $\alpha_n = \sqrt{1 + n^2 - \tau^2}$, $\tau = r_2 k_2$), H_n is the Hankel function of the nth order and first kind with (dropped) argument τ, primes indicate derivatives with respect to the argument, and ξ is defined in Fig. 4.

Focusing on a circular region of radius 35,000 m makes it possible to compare (Fig. 6) the wave height contours resulting from the analytical (above) and the numerical (below) solution. The numerical solution is clearly in good agreement with the analytical one. Please note that these results have been obtained by means of only one iteration, with the values of the angle β calculated at iteration zero being good enough to eliminate spurious reflections at the open boundaries.

Further insight on the quality of the results can be obtained by comparing the analytical and numerical wave height along the island coastline (Fig. 7). The numerical result appears closely to match the analytical solution over almost all the ξ range. Only a small difference is actually visible in the range $0° \leq \xi \leq 20°$.

3.3. Harbor resonance

The 'Harbor resonance test' has become a standard for assessing numerical wave model performances. This consists in calculating the amplification factor at the backwall of the considered bay for several periods of the incoming wave. The amplification factor is defined as half the ratio of the wave height measured at the center of the backwall and the incoming wave height. This factor is, therefore, equal to one in the case of simple stationary waves, whilst it can assume larger values if the wave period is close to a resonating one.

The computational domain used in this test is shown in Fig. 8 and is very similar to that used by Madsen and Larsen (1987). It consists of an outer area 1.00 m wide, which extends 0.13 m from the fully reflecting straight coastline. The investigated bay is 0.30 m long, 0.06 m wide, and 0.26 m deep, and is discretized by a mesh of 1624 nodes and 2960 elements. Waves are generated at a line placed 0.01 m from the upper 'open' boundary. A total absorption condition ($R = 0$) is imposed on the three-side 'open' boundary, which separates the sea region included in the domain from the semi-infinite region that extends

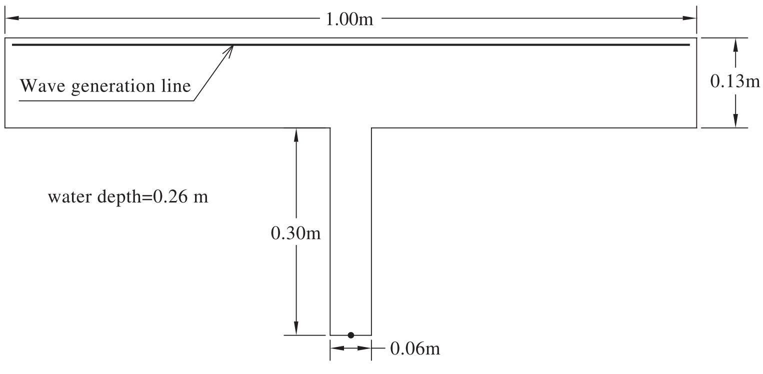

Fig. 8. Computational domain for harbor resonance tests.

outward to infinity. Similarly to the circular island test, the iterative procedure proposed by Beltrami et al. (2001) is used to deal with the angle β indeterminacy of the total absorption condition (Section 2.2), with $\beta = 0$ as initial estimate. On the other hand, a total reflection condition ($R = 1$) is imposed along the coastline and the backwall of the bay, and along the lateral walls.

An analytical solution for this test was presented by Mei (1983, pp. 202–206). According to this solution, which has been derived in the framework of the linear theory, the amplification factor C_a is expressed as:

$$C_a(\omega) = \frac{1}{|Z|} \tag{20}$$

where Z is the bay impedance given by:

$$Z = \cos(kL) + (2k\alpha/\pi)\sin(kL)\ln(2\gamma k\alpha/\pi e) - ik\alpha\sin(kL), \tag{21}$$

where k is the wave number, L is the bay length, α is equal to half the bay width, and $\gamma = 1.78107248$.

The amplification factors obtained by the numerical model are compared with the analytical ones (Fig. 9). The figure shows two sets of numerical results. The first set was obtained without using the iterative technique for the treatment of the angle β indeterminacy. The outgoing waves are therefore assumed to propagate normally to the 'open' boundaries. The second set was obtained by iterating. As in the circular island test, it has been found that only one iteration is necessary to achieve convergence of the results.

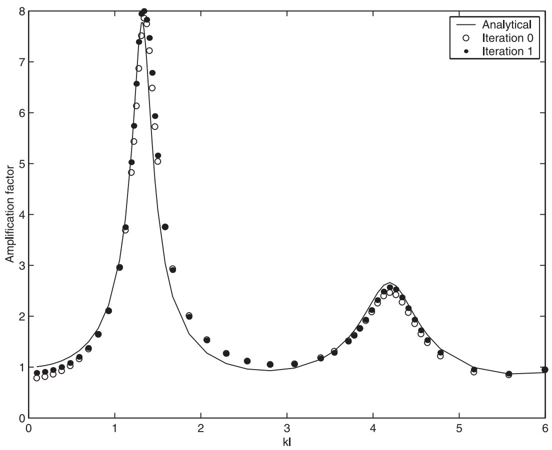

Fig. 9. Amplification factor at the center of the backwall of a long and narrow bay.

4. Discussion and conclusions

The main point of strength of the presented approach is its simplicity. The domain is assumed to be totally contoured by reflecting–absorbing boundaries, a total absorbing condition in particular imposed along the boundary that separates the inner finite from the outer semi-infinite sea region. Sources of energy, which generate waves of the desired height and period, are located within the domain along a line in proximity of the inner–outer sea region boundary. Reflected and scattered waves can propagate over the generation line and are absorbed at the 'open' boundary. In some ways, therefore, the numerical model aims at reproducing the wave paddles and an absorbing device behavior in a physical model. No reflected and scattered wave velocity potential has to be specified along the 'open' boundary, making it possible to elude the difficulties of its mathematical representation (Xu et al., 1996; Zhao et al., 2001) when dealing with sloping bathymetry and when a breaking wave field is to be simulated within the domain.

Minor disadvantages characterize the method. In particular, a larger domain must be used in comparison with that needed by traditional techniques. Providing a suitable mathematical representation of the exterior sea makes it possible with the traditional approach (Berkhoff, 1972, 1976; Chen and Mei, 1974; Mei, 1983, pp. 168–182; Chen and Houston, 1987; Xu et al., 1996) to place the 'open' boundary very close to the scattering objects. In the circular island test, for example, Xu et al. (1996) used a circular domain of radius equal to 35,000 m, whilst a square region of sides equal to 130,000 m has been used in the present case. Furthermore, in the harbor resonance test, the traditional approach makes it possible to discretize a small sea region out of the long and narrow bay, obtaining an almost perfect matching with the analytical solution. As pointed out by Madsen and Larsen (1987), a large exterior domain is necessary to obtain good results when internal wave generation is used in the 'harbor resonance test'. The reduction of the external area leads to a reduction of the amplification afactors.

It is the authors' belief that the traditional approach, which is actually almost perfect when applied for simulating simple geometry cases, should be used with special care when applied to simulate complex wave fields characterized by not well-known scattering and reflection sources as well as by wave breaking. In these latter situations, the proposed approach can represent an attractive alternative solution.

Acknowledgements

This work was partially funded by the MURST (Italian Ministry for Scientific and Technological Research) under the contract "PRIN–Idrodinamica e Morfodinamica di Spiagge Protette da Opere Tracimabili" and by the EU under contract no. EVK-2000-22038 (Delos). We wish to thank Dr. Maurizio Brocchini for carefully reading the manuscript and for useful suggestions.

References

Battjes, J.A., Janssen, J.P.F.M., 1978. Energy loss and set-up due to breaking of random waves. Proceedings of the 16th International Conference on Coastal Engineering. ASCE, New York, USA.

Behrendt, L., 1985. A finite element model for water wave diffraction including boundary absorption and bottom friction. PhD Thesis, ISVA No. 37. Technical University of Denmark, Lyngby, Denmark.

Beltrami, G.M., De Girolamo, P., Bellotti, G., Sammarco, P., 1998. Un modello agli elementi finiti per la risoluzione della 'mild-slope equation' con l'inclusione di un termine dissipativo. XXVI Convegno di Idraulica e Costruzioni Idrauliche, vol. III. CUECM, Cantania, Italy, pp. 193–206. Catania; Settembre 9–12, 1998 (in Italian).

Beltrami, G.M., Bellotti, G., De Girolamo, P., Sammarco, P., 2001. Treatment of wave-breaking and total absorption in a mild-slope equation FEM model. ASCE J. Waterw., Port, Coast. Ocean Eng. 127 (5), 263–271.

Berkhoff, J.C.W., 1972. Computation of combined refraction–diffraction. Proceedings of the 13th International Conference on Coastal Engineering. ASCE, Vancouver, Canada.

Berkhoff, J.C.W., 1976. Mathematical models for simple harmonic linear water waves. Wave Refraction and Diffraction (Publ. 163). Delft Hydraulics Laboratory, Delft, The Netherlands.

Booij, N., 1981. Gravity waves on water with non-uniform depth and current. PhD Thesis. Technical University of Delft, Delft, The Netherlands.

Chen, H.S., 1986. Effects of bottom friction and boundary absorption on water wave scattering. Appl. Ocean Res. 8 (2), 99–104.

Chen, H.S., Houston, J.R., 1987. Calculation of Water Oscillation in Coastal Harbors; HARBS and HARBD User's Manual. Instruction Rep. CERC-87-2. U.S. Army Engineering, Waterway Experiment Station, Vicksburg, MS.

Chen, H.S., Mei, C.C., 1974. Oscillations and Wave Forces in an Offshore Harbour, Rep. No. 190. Department of Civil Engineering, Massachusetts, Institute of Technology, Cambridge, MA.

Copeland, G.J.M., 1985. A practical alternative to the mild-slope wave equation. Coast. Eng. 9, 125–149.

Dally, W.R., Dean, R.G., Dalrymple, R.A., 1985. Wave height variation across beaches of arbitrary profile. J. Geophys. Res. 90 (C6), 11917–11927.

Dalrymple, R.A., Kirby, J.T., Hwang, P.A., 1984. Wave diffraction due to areas of high energy dissipation. ASCE J. Waterw., Port, Coast. Ocean Eng. 110 (1), 67–79.

De Girolamo, P., Sammarco, P., 1993. Analisi teorica di un modello ad elementi finiti per la risoluzione della 'mild-slope equation' con l'inclusione di un termine dissipativo. Atti di Costruzioni Marittime no. 2, DITS, Università di Roma "La Sapienza", Rome, Italy, pp. 1–77. In Italian.

De Girolamo, P., Kostense, J.K., Dingemans, M.W., 1989. Inclusion of wave breaking in a mild-slope model. In: Schrefler, B.A., Zienkiewicz, O.C. (Eds.), Computer Modelling in Ocean Engineering. Balkema, Rotterdam, The Netherlands, pp. 221–229.

Delft Hydraulic Laboratory, 1985a. Documentation Program System PHAROS. Program Harbour Oscillations. Wiskundige Formulering en Struktuur van het Programma. Jannuary (in Dutch).

Delft Hydraulic Laboratory, 1985b. Documentation Program Package PHAROS. Wave Penetration Model. Computation of Combined Refraction Diffraction Effect. User's Guide. Delft Hydraulics, Delft. April.

Demirbilek, Z., Panchang, V., 1998. CGWAVE: A Coastal Surface Water Wave Model of the Mild Slope Equation. Technical Rep. CHL-98-26. U.S. Army Engineering, Waterway Experiment Station, Vicksburg, MS.

Dingemans, M.W., 1997. Water Wave Propagation Over Uneven Bottoms: Part 1. Linear Wave Propagation. World Scientific, Singapore.

Homma, S., 1950. On the behaviour of seismic sea waves around a circular island. Geophys. Mag. 21, 199–208.

Isaacson, M., Qu, S., 1990. Waves in a harbour with partially reflecting boundaries. Coast. Eng. 14, 193–214.

Jonsson, I.G., Skovgaard, O., Brink-Kjaer, O., 1976. Diffraction and refraction calculations for waves incident on an island. J. Mar. Res. 343, 469–496.

Kostense, J.K., Meijer, K.L., Dingemans, M.W., Mynett, A.E., Van den Bosch, P., 1986. Wave energy dissipation in arbitrarily shaped harbours of variable depth. Proceedings of the 20th International Coastal Engineering Conference, pp. 2002–2016.

Larsen, J., Dancy, H., 1983. Open boundaries in short-wave simulations—a new approach. Coast. Eng. 7, 285–297.

Lee, C., Doug Suh, K., 1998. Internal generation of waves for time dependent mild-slope equations. Coast. Eng. 34, 35–57.

Madsen, P.A., Larsen, J., 1987. An efficient finite-difference approach to the mild-slope equation. Coast. Eng. 11, 329–351.

Mei, C.C., 1983. The Applied Dynamics of Ocean Surface and Waves. World Scientific, Singapore.

Mei, C.C., 1995. Mathematical Analysis in Engineering—How to Use the Basic Tools. Cambridge Univ. Press, Cambridge.

Steward, D.R., Panchang, V., 2000. Improved boundary condition for surface water waves. Ocean Eng. 28, 139–157.

Thompson, E.F., Hadley, L.L., 1995. Numerical modeling of harbor response to waves. J. Coast. Res. 11 (3), 744–753.

Thompson, E.F., Chen, H.S., Hadley, L.L., 1996. Validation of numerical model for wind waves and swell in harbors. ASCE J. Waterw., Port, Coast. Ocean Eng. 122 (5), 245–257.

Wei, G., Kirby, J., Sinha, A., 1999. Generation of waves in Boussinesq models using a source function method. Coast. Eng. 36, 271–299.

Xu, B., Panchang, V., Demirbilek, Z., 1996. Exterior reflections in elliptic harbor wave models. ASCE J. Waterw., Port, Coast. Ocean Eng. 122 (3), 118–126.

Zhao, L., Panchang, V., Chen, W., Demirbilek, Z., Chabbra, N., 2001. Simulation of wave breaking effects in two-dimensional elliptic harbor wave models. Coast. Eng. 42, 359–373.